

## **MODEL-REDUCTION METHOD FOR ELECTROMAGNETIC PROBLEMS**

M. A. Kolbehdari

Department of Electronics  
Carleton University  
Ottawa, Ont. K1S 5B6

- 1. Introduction**
  - 2. Basic Formulations**
    - 2.1 Vector Finite Element Formulation
    - 2.2 Complex Frequency Hopping
    - 2.3 Moments-Generation
  - 3. Computational Results**
    - 3.1 Overlap Integrals
  - 4. Conclusions**
- References**

### **1. INTRODUCTION**

Recent research in computational electromagnetics has been widely focused on the development of general-purpose solution methods for electromagnetic problems such as scattering, dielectric cavity resonators, dielectric waveguides, integrated optical waveguides, EMI and EMC studies, VLSI chips and packages, and computer-aided design [1–4]. According to Maxwell's equations, all of the propagating modes within an inhomogeneous structure are hybrid. Therefore, it is necessary to perform full-wave analysis for such structures.

Many numerical methods have been developed in the literature. Typical methods are the mode-matching method [5], the boundary element method [6], the various finite element method [7–9], and frequency-domain finite-difference method [10]. The finite element method is the most generally applicable and most versatile in modeling non-

orthogonal and/or non-uniform grid problem. It is possible to fit any polygonal shape by choosing triangular element shapes and sizes and to increase the accuracy of the solution by using high-order polynomial approximation functions. It is also very suitable for computing electromagnetic fields in inhomogeneous media.

More recently, it was suggested that the edge-elements whose degrees of freedom are associated with the fields along the six edges of a tetrahedron should replace the conventional nodal-based elements [1], with the functional formulation of full magnetic or electric fields to cure the spurious modes problem [11]. In contrast to the node-based elements, edge elements can treat geometries with sharp edges and divergenceless. In the analysis of the modes of inhomogeneous problems using edge-elements, the continuity of electric or magnetic field intensities is imposed across the material interfaces and the continuity of the flux density in the normal direction is satisfied through the natural boundary conditions in the variational process. The reason for the edge-elements to overcome the spurious modes is the improved modeling of the undesired gradient field at zero frequency.

The computational methods of electromagnetic problems in high-speed analog and digital integrated circuits require electromagnetic analysis of the distributed system. A distributed electromagnetic analysis results in a large number of degrees of freedom in the tangential vector finite element model. Consequently, it is necessary to develop a more efficient technique for the solution of the large matrices resulting from numerical methods, but also to develop a reduced-order model which substitutes the mathematical model of the problem with a substantially lower-order but sufficiently accurate model.

More recently, the complex frequency hopping method which has been used efficient in the simulation of large circuits including both lumped elements and transmission lines [12–14] was used in conjunction with the finite element modeling of electromagnetic problems [15, 16]. This paper discusses the extension of a model reduction method [15, 16] based on the tangential vector finite element and complex frequency hopping methods to compute the resonant frequencies of cavity resonators and the characteristic impedance of stripline shielded in a rectangular cavity.

Complex frequency hopping is a technique recently developed in the circuit simulation area, which yields a speed-up factor of 10–1000 over conventional circuit simulators. It has been extended to the solution of

static fields in VLSI interconnects, in ground/power planes and thermal equations [14, 17]. CFH uses the concept of moment matching [18] to obtain both frequency- and time-domain responses of large linear networks through a lower-order multipoint Pade approximation. It extracts a relatively small set of dominant poles to represent a large network that may contain hundreds to thousands of actual poles. CFH is particularly suitable for solving large sets of ordinary differential equations obtained from the FEM analysis of electromagnetic problems. The main advantages of the proposed model-reduction technique can be summarized as follows: (1) 10-1000 times faster than the conventional FEM solution techniques; (2) produces simultaneously both the frequency- and the time-domain results; (3) can handle general cases of electromagnetic problems; both nodal and edge element formulations; (4) the solution algorithm does not suffer from the instability problems associated with conventional methods; (5) problems consisting of Dirichlet, Neumann and combined boundary conditions can be solved and the proposed model-reduction technique can be easily integrated with conventional electromagnetic simulators.

The following sections describe the steps involved in this method: the field formulations of the problem are given in Section 2; in subsections A, B, and C the tangential vector finite element method, complex frequency hopping, and moment generation are discussed. In Section 3, computational results are presented; finally a brief conclusion is given in Section 4.

## 2. BASIC FORMULATIONS

Efficient three-dimensional full wave analysis (FWA) of electromagnetic problems becomes more important when one needs to accurately characterize the dispersive properties of high-speed digital or analog devices at higher frequencies. FWA takes into account all field components and related boundary conditions. TVFEM is nowadays a basic technical instrument for electrical engineers; its rapid success is due to a steadily increasing availability of computer programs that can be used without any difficulties.

An electromagnetic wave propagation phenomenon can be expressed by the Maxwell's coupled curl equations as

$$\frac{1}{\mu_r} \nabla \times \mathbf{E} = -j\omega\mu_o \mathbf{H} \quad (1a)$$

$$\nabla \times \mathbf{H} = j\omega\epsilon\mathbf{E} + \mathbf{J}^i \quad (1b)$$

where the harmonic variation  $\exp(j\omega t)$  is assumed.  $\mathbf{H}$  denotes the magnetic field vector,  $\mathbf{E}$  the electric field,  $\mathbf{J}^i$  the current density,  $\mu$  the permeability,  $\epsilon$  the permittivity of the material, and  $\omega$  the angular frequency of the electromagnetic phenomenon. Eliminating  $\mathbf{H}$  from equations (1a) and (1b) yields the following TVFEM's equations

$$\nabla \times \frac{1}{\mu_r} \nabla \times \mathbf{E} - \mathbf{k}_o^2 \epsilon_r \mathbf{E} = -j\omega\mu_o \mathbf{J}^i \quad \text{in } \Omega \quad (2a)$$

$$\mathbf{n} \times \mathbf{E} = 0 \quad \text{on } \Gamma_e \quad (2b)$$

$$\mathbf{n} \times \nabla \times \mathbf{E} = 0 \quad \text{on } \Gamma_h \quad (2c)$$

$$\nabla \times \mathbf{E} = jk_o \mathbf{E} \quad \text{on } \Gamma_s \quad (2d)$$

where  $\Gamma_e$ ,  $\Gamma_h$  are perfect electric and magnetic surfaces, respectively, inside  $\Omega$ ,  $\Gamma_s$  is the truncation boundary,  $\mathbf{n}$  is the unit vector normal on these surfaces,  $k_o^2 = \omega^2 \mu_o \epsilon_o$ ,  $\mu_o$  and  $\epsilon_o$  are the permeability and permittivity of the free space, respectively, and  $\epsilon_r = \frac{\epsilon}{\epsilon_o}$ . For the sake of simplicity, the first-order absorbing boundary condition on  $\Gamma_s$  is selected to truncate the infinite domain into a finite region. Using Galerkin's method [19], the bilinear functional for the electric field is

$$\begin{aligned} F(\mathbf{E}^t, \mathbf{E}) &= \int_V \left( \frac{1}{\mu_r} \nabla \times \mathbf{E}^t \right) \bullet (\nabla \times \mathbf{E}) - \mathbf{k}_o^2 \epsilon_r \mathbf{E}^t \bullet \mathbf{E} + j\omega\mu_o \mathbf{E}^t \bullet \mathbf{J}^i \, d\mathbf{v} \\ &\quad + jk_o \int_{\Gamma_s} \mathbf{E}^t \bullet (\mathbf{E} \times \mathbf{n}) \, ds \\ &= 0 \end{aligned} \quad (3)$$

where  $\mathbf{E}^t$  is a testing function.

## 2.1 Vector Finite Element Formulation

The formulation based on the tangential vector finite element method and absorbing boundary condition is presented. The entire problem domain is discretized into a finite number of subregions called elements. The Galerkin's finite element procedure is applied to formulate the bounded region. The extension of a finite element to open boundaries is carried out by imposing Sommerfeld's radiation condition.

In the tangential vector finite element formulation, the problem domain,  $V$ , is subdivided into tetrahedral elements,  $V^e (e = 1, 2, \dots, M)$ ,

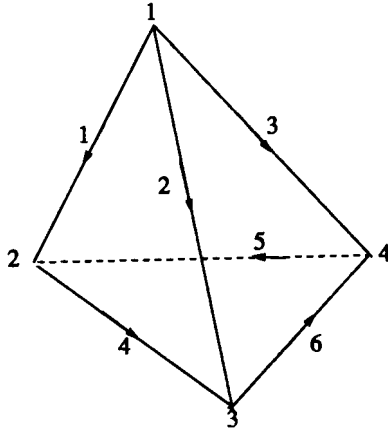


**Figure 1.** Node and edge numbering of the tetrahedral element.

where  $M$  denotes the total number of tetrahedral elements. The three-dimensional edge-based,  $W_j^e$ , the Whitney 1-form vector shape function associated to the  $j$ -th edge between nodes  $j1$  and  $j2$  is defined in the tetrahedrons as

$$\mathbf{W}_j^e = l_j^e (L_{j1}^e \nabla L_{j2}^e - L_{j2}^e \nabla L_{j1}^e) \quad (4)$$

where  $L_{j1}$  and  $L_{j2}$  are the barycentric functions [20] of node  $j1$  and  $j2$  and  $l_j$  is the length of a tetrahedron edge. The edge and node numbering scheme used is shown in Fig. 1 and Table I. Over each tetrahedral element of the problem domain,  $V$ , the  $\mathbf{E}$ -field is expressed in terms of the linear basis function as

$$\mathbf{E} = \sum_{i=1}^6 E_i^e \mathbf{W}_i^e \quad (5)$$

where  $E_i$  represents the tangential  $\mathbf{E}$ -field on the element edges. The basis functions used in this analysis have zero divergence and constant curl.

Edge $j$	Node $j1$	Node $j2$
1	1	2
2	1	3
3	1	4
4	2	3
5	4	2
6	3	4

**Table I.** Edge numbering order on a tetrahedral element

Applying the Galerkin's method results in the weak form formulation which can be written as a matrix equation

$$[\mathbf{A} + jk_o\mathbf{B} - k_o^2\epsilon_r\mathbf{C}][E] = -j\omega\mu_o\mathbf{D} \quad (6a)$$

Equation (6a) can be re-written as

$$\mathbf{Y}(s)\mathbf{X}(s) = \mathbf{R}(s) \quad (6b)$$

The element matrices in (6a) are defined as

$$\mathbf{A}_{ij}^e = \int_{V^e} (\nabla \times \mathbf{W}_i^e) \bullet \left( \frac{1}{\mu_r} \nabla \times \mathbf{W}_j^e \right) dv \quad (7a)$$

$$\mathbf{B}_{ij}^e = \int_{S^e} \mathbf{W}_i^e \bullet (\mathbf{W}_j^e \times \mathbf{n}) ds \quad (7b)$$

$$\mathbf{C}_{ij}^e = \int_{V^e} \mathbf{W}_i^e \bullet \mathbf{W}_j^e dv \quad (7c)$$

$$\mathbf{D}_i^e = \int_{V^e} \mathbf{W}_i^e \bullet \mathbf{J} dv \quad (7d)$$

where  $V^e$  is the elemental volume;  $S^e$  is the elemental surface.

## 2.2 Complex Frequency Hopping

Complex frequency hopping (CFH) [12–14] is a recently developed model-reduction algorithm in the circuit simulation area. It has been successfully and efficiently applied to the solution of large set of ordinary differential equations and it uses moment-matching to obtain a reduced-order model of a linear system. In general, the moment matching technique approximates the frequency response of a Taylor series

expansion in the complex  $s$  plane. The cost of an expansion is approximately one frequency point analysis. The moments (coefficients of the expansion) are matched to a lower-order transfer function using a rational Pade approximation. This transfer function can be used to obtain the output response. Single Pade approximations are accurate near the point of expansion in the complex  $s$  plane and decrease in accuracy with increased distance from the point of expansion. CFH overcomes this problem by performing multiple Taylor expansions in the complex plane using a binary search algorithm. With a minimized number of frequency point expansions, enough information is obtained to enable the generation of an approximate transfer function that matches the original function up to a pre-defined highest frequency. The transfer function or set of transfer functions then acts like the entire network up to that frequency, in both the time and frequency domains.

Expanding  $\mathbf{X}(s)$  in (6b) about the complex frequency point  $s = \alpha$  yields,

$$\mathbf{X}(s) = \sum_i \mathbf{M}_n (s - \alpha)^n \quad (8)$$

where  $\mathbf{M}_n$  is the  $n^{\text{th}}$  vector of coefficients (moments) of the Taylor series expansion. A recursive relation for the evaluation of moments can be obtained in the form

$$[\mathbf{Y}(\alpha)]\mathbf{M}_n = - \sum_{r=1}^n \frac{\mathbf{Y}(s)^{(r)}|_{s=\alpha} \mathbf{M}_{n-r}}{r!} \quad (9)$$

The transfer function of the system is then found by matching a Pade approximation to the moments of the system in (8). The reduced-order model which is obtained in terms of approximate dominant poles  $\hat{p}_i$  and residues  $\hat{k}_i$  of the system can be represented as

$$H(s) = \hat{H}(s) = \hat{c} + \sum_{i=0}^L \frac{\hat{k}_i}{s - \hat{p}_i} \quad (10)$$

where  $\hat{c}$  is the direct coupling constant between the input and the output and  $L$  is the total number of dominant poles extracted. The corresponding approximate time-domain impulse response is given by

$$h(t) = \hat{h}(t) = \hat{c}\delta t + \sum_{i=0}^L \hat{k}_i e^{\hat{p}_i t} \quad (11)$$

In order to compute the moments in (9), we need the derivatives  $\mathbf{Y}^{(r)}(s)$ . The computation of  $\mathbf{Y}^{(r)}(s)$  has been discussed extensively in the circuit simulation area where the  $\mathbf{Y}(s)$  matrix comprises circuit elements such as inductors/capacitors and quasi-TEM interconnect models. However, the computation of these moments in the case of electromagnetic formulations has not been addressed previously in the literature. In the following section we propose an efficient method to compute these derivatives for EM formulations.

### 2.3 Moments-Generation

To obtain the derivatives of  $\mathbf{Y}(s)$  in (9), a recursive relationship has been developed and is summarized below:

$$[\mathbf{C}\alpha^2 + \mathbf{B}\alpha + \mathbf{A}]\mathbf{M}_0 = \mathbf{R}(\alpha) \quad (12)$$

$$[\mathbf{C}\alpha^2 + \mathbf{B}\alpha + \mathbf{A}]\mathbf{M}_1 = -[\mathbf{B} + 2\alpha\mathbf{C}]\mathbf{M}_0 + \mathbf{R}'(\alpha) \quad (13)$$

$$[\mathbf{C}\alpha^2 + \mathbf{B}\alpha + \mathbf{A}]\mathbf{M}_n = -\mathbf{B}\mathbf{M}_{n-1} - \mathbf{C}[2\alpha\mathbf{M}_{n-1} + \mathbf{M}_{n-2}] + \frac{\mathbf{R}^n(\alpha)}{n} \quad (14)$$

for  $n \geq 2$ . Here (12), (13) and (14) give the system moments recursively at a given expansion point  $s = \alpha$ .

## 3. COMPUTATIONAL RESULTS

Numerical examples involving formulations for the case of homogeneous structures are presented in [15]. In this paper three numerical examples are given to demonstrate the applicability and the speed-up achieved in the case of inhomogeneous structures arising in electromagnetic problems. The accuracy and efficiency of the proposed method were examined for the resonant frequencies of a rectangular cavity and conical cavity with a dielectric rod filling exciting with a Gaussian pulse current vector and a stripline shielded in a rectangular cavity. These examples were performed on Sun Sparc 5 workstation.

Example 1: In this example the resonant frequencies of an empty rectangular cavity of dimension:  $a = 1.5m$ ,  $b = 1.2m$ , and  $c = 1.0m$  shown in Fig. 2 are evaluated using the proposed model-reduction technique. This example was discretized with 1912 tetrahedrons, 2431 edges, and 1829 unknowns. Using a similar kind of discretization and equations (12)-(14), the required moments are generated and the resonant frequencies are extracted using the CFH algorithm. In Table II,

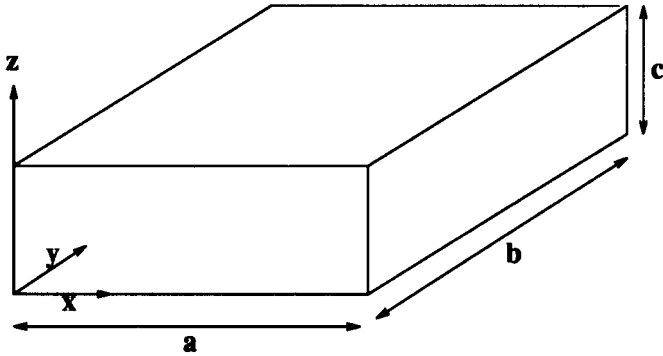


**Figure 2.** A rectangular waveguide cavity.

the resonant frequencies obtained using the proposed model-reduction technique and the conventional FEM frequency-domain (FEMFD) approaches are given and they match accurately. Also, the resonant frequencies obtained using the proposed technique are compared with the analytical solution and they agree reasonably. The speed-up achieved using the proposed technique is compared to FEMFD in Table III.

Mode	FEM & CFH GHz	FEMFD GHz	Analytical GHz
110	159.77	159.34	160.07
101	180.21	180.08	180.11
011	194.29	194.37	195.29
111	219.51	219.67	219.51
210	234.46	234.47	235.76
201	250.38	250.22	250.09
102	317.11	317.23	316.21
120	268.19	268.22	269.39
121	309.21	309.21	308.31

**Table II** Comparison of resonant frequencies.

<b>Matrix Size</b>	<b>FEM &amp; CFH Minutes</b>	<b>FEMFD Minutes</b>	<b>Speed-up Ratio</b>	<b>No. of Hops</b>
1829 × 1829	7.75	923.8	125	13
2011 × 2011	10.61	1126.7	106	15

**Table III** CPU Time Comparison.

Example 2: In this example a conical cavity with a dielectric rod filling is considered, as shown in Fig. 3. This was also studied in [21] chosen to demonstrate the accuracy and CPU speed-up of the proposed method. The finite element mesh consisted of 3432 tetrahedrons with 4531 edges and 3412 unknowns. The structure is analyzed using the proposed technique and the resonant frequencies are evaluated. Table IV gives the accuracy comparison of the proposed technique with the conventional FEMFD approach and the results reported in [21]. The results match accurately. The speed-up achieved using the proposed technique is compared to FEMFD in Table V.

<b>Mode</b>	<b>FEM &amp; CFH GHz</b>	<b>FEMFD GHz</b>	<b>Ref. [21] GHz</b>
010	1.521	1.520	1.491
110	2.479	2.471	2.430
111	2.511	2.509	2.501
011	3.041	3.031	3.011
210	3.281	3.272	3.211
011	3.399	3.401	3.312
211	3.439	3.428	3.411
020	3.599	3.588	3.571
121	3.841	3.831	3.801

**Table IV** Comparison of resonant frequencies.

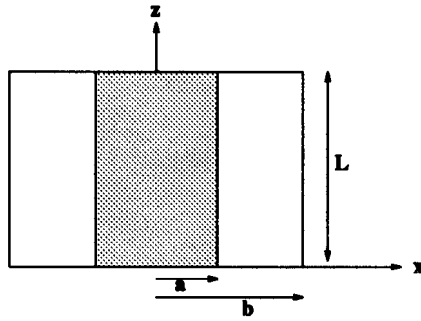


**Figure 3.** Cylindrical cavity;  $a = 1.00075$  cm,  $b = 1.27$  cm,  $L = 1.397$  cm,  $\epsilon = 37.6$ .

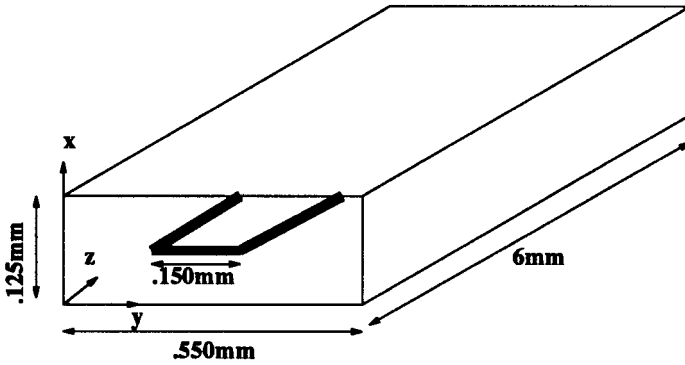


**Figure 4.** Stripline shielded in rectangular cavity.

Matrix Size	FEM & CFH Minutes	FEMFD Minutes	Speed-up Ratio	No. of Hops
$3412 \times 3412$	22.01	1534.1	69	19
$3721 \times 3721$	26.25	1875.2	58	21

**Table V** CPU Time Comparison.

Example 3: This example consists of stripline shielded in a rectangular cavity, shown in Fig. 4 chosen [22] for the purpose of demonstrating the accuracy and CPU speed-up of the proposed model-reduction technique. The structure is analyzed using the proposed technique and the characteristic impedances are evaluated. Table VI gives the accuracy comparison between the proposed technique with the conventional FEMFD approach and the results reported in [22]. The results match accurately. The speed-up achieved using the proposed technique is compared to FEMFD in Table VII. The stripline used in packaging applications typically will not have side walls. Here it is used to illustrate the proposed method. The line is excited with the field distribution varying sinusoidally in time at a frequency which is below the cut-off of the higher order mode in the waveguide. The front and back of the waveguide are truncated using absorbing boundary conditions. The voltage and current at a sampling point are calculated from the field computation following the procedure outlined below. The voltage is determined by performing a line integral of the dielectric field from one of the walls to the stripline as

$$V = \int_a^b \mathbf{E} \cdot d\mathbf{l} \quad (15)$$

The current is calculated by a closed line integral of the magnetic field around the strip as

$$I = \int_c \mathbf{H} \cdot d\mathbf{l} \quad (16)$$

where the contour,  $c$ , is a boundary enclosing the strip.

<b>Freq. GHz</b>	<b>FEM &amp; CFH Ohm</b>	<b>FEMFD Ohm</b>	<b>Ref. [22] Ohm</b>
40	35.51	35.51	35.62
50	35.88	35.85	35.90
60	36.11	36.01	36.24
70	36.20	36.13	36.45
80	36.42	36.41	36.67
90	36.62	36.65	36.72
100	37.14	37.16	37.23
110	37.81	37.65	37.92
120	38.25	38.25	38.45

**Table VI** Comparison of characteristic impedances.

<b>Matrix Size</b>	<b>FEM &amp; CFH Minutes</b>	<b>FEMFD Minutes</b>	<b>Speed-up Ratio</b>	<b>No. of Hops</b>
2412 × 2412	15.01	1134.1	75	15
2721 × 2721	19.25	1375.2	72	17

**Table VII** CPU Time Comparison.

#### 4. CONCLUSIONS

An efficient model-reduction technique based on CFH and FEM for the solution of electromagnetic problems arising in dielectric cavity resonators and stripline is presented in this paper. Examples were analyzed using the proposed technique and compared with analytical and/or other reported results. Reasonable accuracy and a speed-up of two orders of magnitude are achieved compared to conventional techniques. The proposed model-reduction technique yields both frequency- and time-responses and can be easily integrated with conventional electromagnetic simulators.

## References

1. Bossavit, A., and I. Mayergoyz, "Edge-elements for scattering problems," *IEEE Magnetics*, Vol. 25, No. 4, 2816–2821, July 1989.
2. Lee, J. F., "Finite element analysis of lossy dielectric waveguides," *IEEE Microwave Theory Tech.*, Vol. 42, No. 6, 1025–1031, June 1994.
3. Itoh, T., "Spectral domain immittance approach for dispersion characteristics of generalized printed transmission lines," *IEEE Microwave Theory Tech.*, Vol. 28, 733–736, July 1980.
4. Mur, G., "The finite-element modeling of three-dimensional electromagnetic fields using edge and nodal elements," *IEEE Antennas and Propagation*, Vol. 41, No. 7, 948–953, July 1993.
5. Zaki, K. A., and C. Chen, "New results in dielectric-loaded resonators," *IEEE Microwave Theory Tech.*, Vol. 40, 120–127, Jan. 1992.
6. Collin, R. E., and D. A. Ksienshi, "Boundary element method for dielectric resonators and waveguides," *Radio Sci.*, Vol. 22, No. 2, 1155–1167, Dec. 1987.
7. Daly, P., "Hybrid-mode analysis of microstrip by finite-element methods," *IEEE Microwave Theory Tech.*, Vol. 19, 19–25, Jan. 1971.
8. Rahman, B. M. A., and J. B. Davies, "Finite-element analysis of optical and microwave waveguide problems," *IEEE Microwave Theory Tech.*, Vol. 32, 20–28, Jan. 1984.
9. Hano, M., "Vector finite-element solution of anisotropic waveguides using novel triangular elements," *Electronics and Communications in Japan*, Part 2, Vol. 11, 71–80, 1988.
10. Taflove, A., and M. E. Brodwin, "Numerical solution of steady state electromagnetic scattering problems using the time-dependent Maxwell's equations," *IEEE Microwave Theory Tech.*, Vol. 23, 623–630, Aug. 1975.
11. Cendes, Z. J., D. Hudak, J. F. Lee, and D. K. Sun, "Development of new methods for predicting the bistatic electromagnetic scattering from absorbing shapes," *RADC-TR R&D* final report, Carnegie Mellon University.
12. Chiprout, E., and M. S. Nakhla, "Analysis of interconnect networks using complex frequency hopping," *IEEE Trans. CAD*, Vol. 14, No. 2, 186–199, Feb. 1995.
13. Chiprout, E., and M. S. Nakhla, *Asymptotic Waveform Evaluation and Moment Matching for Interconnect Analysis*, Kluwer Academic Publishers, Boston, 1993.

14. Sanaie, R., E. Chiprout, M. S. Nakhla, and Q. J. Zhang, "A fast method for frequency and time domain simulation of high-speed VLSI interconnects," *IEEE Trans. Microwave Theory Tech.*, Vol. 42, No. 12, 2562–2571, Dec. 1994.
15. Kolbehdari, M. A., M. Srinivasan, M. Nakhla, Q. J. Zhang and R. Achar, "Simultaneous time and frequency domain solutions of EM problems using finite element and CFH techniques", *IEEE Trans. Microwave Theory Tech.*, Vol. 44, 1526–1534, Sept. 1996.
16. Kolbehdari, M. A. and M. S. Nakhla, "Reduced-order methods for dielectric resonators using FEM and CFH," submitted to *COMPEL*, Aug. 1997.
17. Liu, D. G., V. Phanilatha, Q. J. Zhang and M. S. Nakhla, "Asymptotic thermal analysis of electronic packages and printed circuit boards", *IEEE Trans. CPMT*, Part A, Vol. 18, 781–787, 1995.
18. Pillage, L. T., and R. A. Rohrer, "Asymptotic waveform evaluation for timing analysis," *IEEE Trans. CAD*, Vol. 9, 352–366, Apr. 1990.
19. Strang, G. and G. F. Fix, *An Analysis of the Finite-Element Method*, Englewood Cliffs, NJ: Prentice-Hall, 1973.
20. Bossavit, A., "Whitney forms: a class of finite elements for three-dimensional computations in electromagnetism," *IEE Proc.*, Part A, Vol. 135, No. 8, 493–500, Nov. 1988.
21. Taheri, M., and D. M. Syahkal, "Accurate determination of modes in dielectric-loaded cylindrical cavities using a one-dimensional finite element method," *IEEE Trans. Microwave Theory Tech.*, Vol. 37, No. 10, 1535–1541, Oct. 1989.
22. Gupta, K. C., R. Grag, and R. Chadha, *Computer-Aided Design of Microwave Circuits*, 63, Artech House, Dedham, MA, 1981.